Microscopic Simulation of a Hydrogen Plasma

J. P. Hansen and I. R. McDonald
Laboratoire de Physique Théorique des Liquides, Equipe associée au Centre National de la Recherche Scientifique, Université Pierre et Marie Curie, 75320 Paris Cedex 05, France
(Received 29 August 1978)

Results are reported of a molecular-dynamics simulation of a semiclassical two-component plasma in the strong-coupling regime. Static and dynamic properties are discussed, with emphasis laid on the collective motion and its description in terms of the spectra of charge fluctuations and the frequency-dependent dielectric function.

There has been much recent progress in our understanding of the microscopic dynamics in strongly coupled Coulombic fluids. Molecular-dynamics (MD) computer simulations of classical one-component plasmas (OCP) in a uniform background,[1] ionic mixtures,[2] molten salts,[3] and ionic superconductors[4] have yielded a wealth of information on single-particle and collective motion in ionic systems. At the same time a number of exact results describing the general features of the collective modes in one- and two-component Coulombic fluids have been derived in the framework of kinetic theory.[5] In this Letter we report on results obtained from a MD simulation of a fully ionized, highly correlated hydrogen plasma, i.e., a two-component system consisting of equal numbers of protons (p) and electrons (e). Such a system cannot be treated wholly classically, since the proton-electron attraction leads to a collapse. We therefore replace the bare Coulomb interactions by two-body effective potentials[6]

$$v_{\alpha\beta}(r) = \pm (e^2/r)(1-\exp\{-r/\lambda_{\alpha\beta}\}), \qquad \alpha,\beta = p,e, \tag{1}$$

where $\lambda_{\alpha\beta}$ is the de Broglie thermal wavelength for the pair α,β; this takes approximate account of quantum diffraction effects at short distances. There is some arbitrariness in our choice, but we do not expect the dynamics of the plasma to be sensitive to details of the short-range behavior of the potentials.

The equilibrium state of the system is characterized by the dimensionless quantities $r_s = a/a_0$ and $\Gamma = e^2/ak_BT$, where $a^3 = 3/4\pi\rho$ ($\rho = N/V$ being the number of electrons per unit volume) and a_0 is the Bohr radius. The simulation was carried out for $r_s = 1$ and $\Gamma = 2$, i.e., $\rho \simeq 1.6\times10^{24}$ cm^{-3} and $k_BT = 1$ Ry ($T \simeq 160\,000$ K). These are conditions under which hydrogen is fully ionized but where quantum effects should not be too severe, since $\lambda_{\alpha\beta} < a$ for all α,β. Because the ratio of the Debye screening length to the ion-sphere radius [$\Lambda_D/a = (6\Gamma)^{-1/2} \simeq 0.3$] is considerably less than one we are clearly in the strong-coupling regime, i.e., the interaction energy is comparable with or greater than the thermal energy. As a description of high-density plasmas, such as those produced by laser implosion, the present model is more realistic than the OCP, where the role of one of the constituents is reduced to that of a uniform background. It becomes equivalent to the OCP in the limit of vanishing electron mass; the electrons then form either a classical ($\hbar = 0$) or degenerate ($\hbar = 0$) ideal-gas background.

We have used the standard MD technique (handling the Coulombic interactions by an Ewald transformation[7]) to solve numerically the equations of motion of 125 protons and 125 electrons. The large proton-to-electron mass ratio means that two different time scales are involved, the characteristic frequencies for the two species being the electron plasma frequency $\Omega_p = (3e^2/m_ea^3)^{1/2}$ and the proton plasma frequency $\omega_p = (3e^2/m_pa^3)^{1/2}$. The choice of time step in the numerical integration is of course dictated by the *electronic* motion; in practice we have adopted the value $\Delta t = 0.08\Omega_p^{-1} \simeq 10^{-18}$ sec. Two independent simulations were carried out, each extending over $24\,000\Delta t$. Thus each run covered approximately 2000 electron plasma oscillations but only 50 proton plasma oscillations; the statistics on the electronic motion are therefore correspondingly greater. Though the mass ratio is large, we experienced no particular difficulty in either reaching or maintaining equilibrium. For the purpose of comparison we have, in addition, carried out a simulation of the OCP, of similar length and for the same value of Γ.

We mention first a number of results on static properties. The three partial pair distribution functions $g_{\alpha\beta}(x)$, plotted in Fig. 1 as functions of $x = r/a$, show all the expected qualitative features; they also agree well with results obtained by solving the three coupled hypernetted-chain (HNC) equations,[3] except that HNC theory somewhat underestimates the peak in $g_{pe}(x)$ at $x = 0$. There is

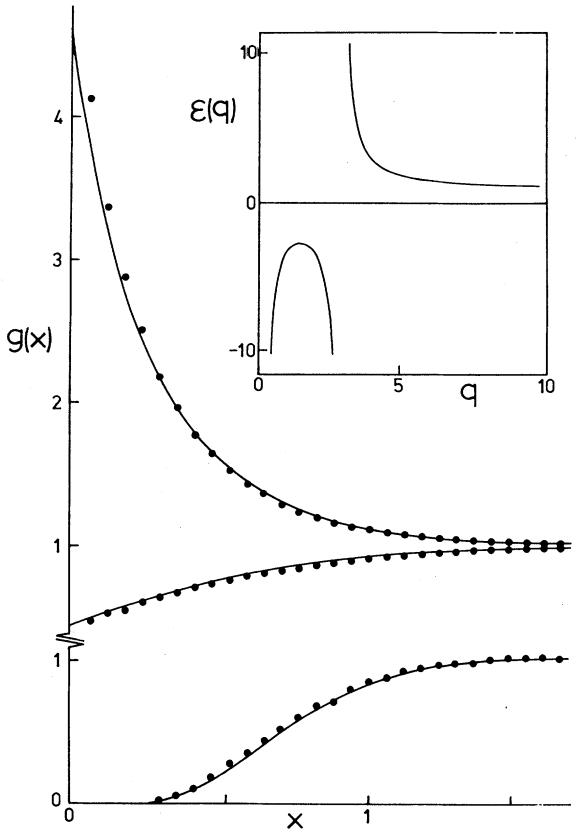

FIG. 1. $g_{\alpha\beta}(x)$ as functions of x. Reading from top to bottom, $g_{pe}(x)$, $g_{ee}(x)$, and $g_{pp}(x)$. Points, MD; curves, HNC. Note the break in vertical scale. Inset: static dielectric constant.

a corresponding difference in the pressures calculated from the virial theorem, from which we find $PV/2Nk_BT = 0.63$ (MD), i.e., $P \simeq 22$ Mbar, and 0.74 (HNC). By forming the appropriate linear combination of partial structure factors [the Fourier transforms of $g_{\alpha\beta}(x)$], we obtain the charge-charge structure factor $S_{zz}(q)$. The static dielectric constant $\epsilon(q)$ can then be calculated from the expression

$$1/\epsilon(q) = 1 - (6\Gamma/q^2)S_{zz}(q), \tag{2}$$

where $q = ak$ is a dimensionless wave number. From Fig. 1 we see that $\epsilon(q)$ is negative for $q \lesssim 3$, behavior which reflects the importance of interparticle correlations.

To study the dynamics of the plasma we have

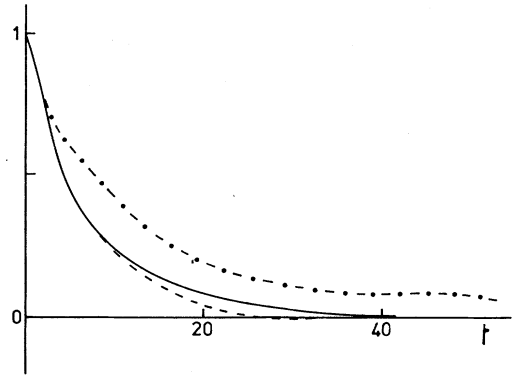

FIG. 2. Velocity and charge current acf's. Full curve, $Z_e(t)$; dashes, $Z_p(t)$; dash-dotted, $J(t)$. Unit of t is Ω_p^{-1} for $Z_e(t)$ and $J(t)$ and ω_p^{-1} for $Z_p(t)$.

computed a number of time-dependent autocorrelation functions (acf's) and their spectra. In Fig. 2 we show the two velocity acf's $Z_p(t)$, $Z_e(t)$ and the microscopic charge-current acf $J(t)$, the integrals of which yield, respectively, the self-diffusion coefficients D_p, D_e and the electrical conductivity σ. The velocity acf's are similar in shape, scaling in time roughly as $(m_p/m_e)^{1/2}$, but $J(t)$ is much longer lived. There is consequently an enhancement of σ by a factor of approximately 2 relative to that predicted by a naive Nernst-Einstein relation

$$\sigma = \tfrac{1}{2}(Ne^2/Vk_BT)(D_p + D_e), \tag{3}$$

whereas similar calculations[3] for a molten salt show that cooperative effects lead in that case to a *negative* deviation from the Nernst-Einstein relation of approximately 20%. Integration of the curves plotted in Fig. 2 gives $D_p/a^2\omega_p = 1.01$, $D_e/a^2\Omega_p = 1.23$, and $\sigma/\Gamma\Omega_p = 0.30$; for the OCP at $\Gamma = 2$ we find[1] that $D/a^2\omega_p = 0.87$, in fair agreement with the present result for D_p.

The collective dynamical modes can be described in terms of fluctuations in the microscopic partial densities

$$\rho_\alpha(\vec{q}, t) = \sum_{j=1}^{N} \exp\{-i\vec{q}\cdot\vec{r}_{j\alpha}(t)\}, \quad \alpha = p, e. \tag{4}$$

In particular, the spectrum of charge-density fluctuations is given by the Fourier transform of the charge-density acf, i.e.,

$$S_{zz}(q,\omega) = \frac{1}{4\pi N}\int_{-\infty}^{\infty} dt\, e^{i\omega t}\langle\{\rho_p(\vec{q},t) - \rho_e(\vec{q},t)\}\{\rho_p(-\vec{q},0) - \rho_e(-\vec{q},0)\}\rangle \tag{5}$$

with analogous expressions for $S_{pp}(q,\omega)$ and $S_{ee}(q,\omega)$. In Fig. 3 we show results obtained for $S_{zz}(q,\omega)$ at the four smallest wave numbers compatible with the periodic boundary conditions used in the MD calculations. At $q=0.780$ there is a sharp optic-type peak at a frequency slightly above Ω_p. This is a manifestation of the propagating charge relaxation mode characteristic of two-component plasmas, whereas the peak around $\omega=0$ is linked to heat conduction and interspecies energy relaxation.[5] The optic peak broadens rapidly with increasing q, the central peak becoming much more pronounced. The dispersion of the optic peak is difficult to determine, but appears to be weakly negative. On the same graph we show selected results for $S_{ee}(q,\omega)$. At small q there is again an optic peak, much weaker in intensity but of almost identical shape to that seen in $S_{zz}(q,\omega)$, with a correspondingly stronger central peak (not shown). Thus the electron density fluctuations at sufficiently small q are dominated by the thermal mode and interspecies relaxation, whereas charge relaxation contributes most of the intensity in $S_{zz}(q,\omega)$. Some comparison with results for the OCP is also made. The agreement is only qualitative, since the spectra for the OCP are significantly sharper, lack the central peak, and show a strong positive dispersion of the optic peak. For the reasons already indicated, our data are insufficiently precise to yield reliable results on $S_{pp}(q,\omega)$.

Apart from direct observation, the characteristic frequency $\omega(q)$ of the optic mode can also be estimated by standard sum-rule arguments. Expressing the frequency moments $\langle\omega^n(q)\rangle$ of $S_{zz}(q,\omega)$ in terms of $g_{\alpha\beta}(x)$, we find in particular that the estimate given by

$$\omega(q)=(\langle\omega^4\rangle/\langle\omega^0\rangle)^{1/4}=(\langle\omega^4\rangle/S_{zz}(q))^{1/4} \tag{6}$$

increases rapidly with q for $\Gamma<2$, in agreement with mean-field predictions, but *decreases* for $\Gamma\gtrsim 2$. Similar behavior is observed for the OCP.[1] Note that $\omega(q=0)$ exceeds Ω_p by a few percent, as can be inferred from Fig. 3.

Finally, the fluctuation-dissipation theorem[8] connects $S_{zz}(q,\omega)$ with the imaginary part of the charge response function $\chi(q,\omega)$ in the form $k_B T\chi''(q,\omega)=-\pi\omega S_{zz}(q,\omega)$. The real part can then be determined via a Kramers-Kronig relation and the results used to determine the dielectric function $\epsilon(q,\omega)$ from

$$\frac{1}{\epsilon(q,\omega)}=1+(q_D/q)^2 k_B T\chi(q,\omega), \tag{7}$$

where $q_D^2=a^2/\Lambda_D^2=6\Gamma$. The real and imaginary parts of $\epsilon(q,\omega)$ obtained in this way are plotted in

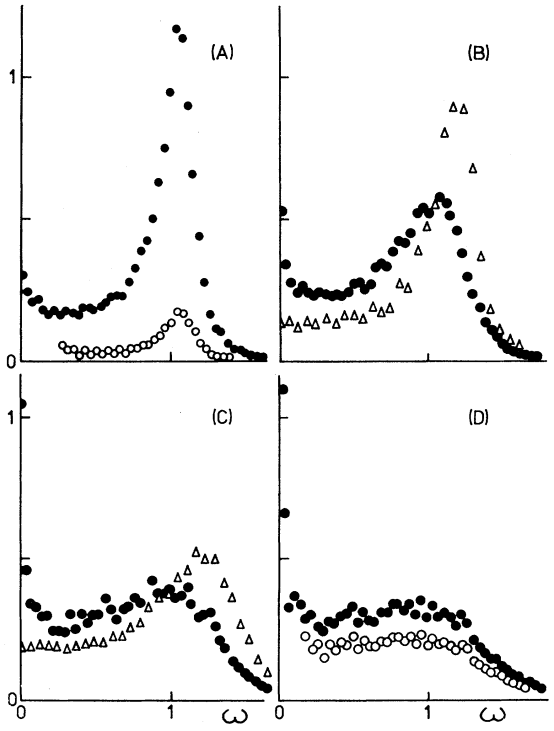

FIG. 3. $S_{zz}(q,\omega)$ (dots) as function of ω (in units of Ω_p) for (a) $q=0.780$, (b) 1.102, (c) 1.350, and (d) 1.559. Circles show $S_{ee}(q,\omega)$ and triangles show $S_{zz}(q,\omega)$ for the OCP at $q=1.072$ (b) and 1.383 (c).

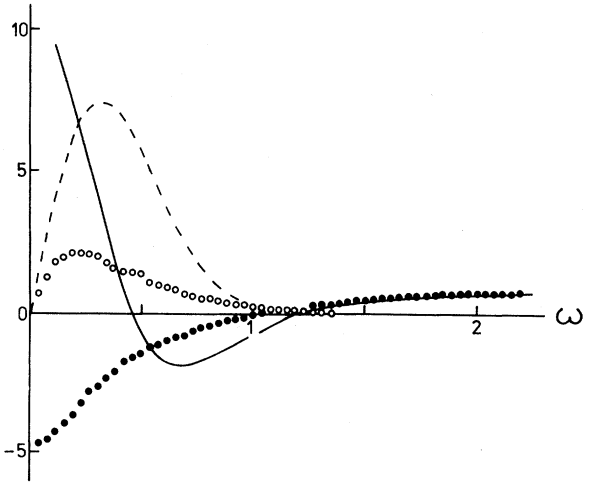

FIG. 4. Complex dielectric function for $q=0.780$. Points, MD; curves, Vlasov. Real part, full curve and dots; imaginary part, dashes and circles. Unit of frequency is Ω_p.

Fig. 4; for $\omega \lesssim \Omega_p$ we see that there is not even qualitative agreement with the standard mean-field (Vlasov) result, particularly in the behavior of $\epsilon'(q,\omega)$ at low frequencies.

Our results indicate that a simulation of the microscopic behavior of a hydrogen plasma is feasible and yields quantitatively meaningful results; the latter indicate that the OCP is only moderately successful in modeling the real plasma. In future work we plan to extend the calculations in three main directions: (i) the computation of transport coefficients, including thermal conductivity; (ii) the incorporation of external magnetic and high-frequency electromagnetic fields; and (iii) the study of nonequilibrium (two-temperature) plasmas.

We thank C. Deutsch for valuable discussions.

[1]J. P. Hansen, I. R. McDonald, and E. L. Pollock, Phys. Rev. A 11, 1025 (1975).
[2]I. R. McDonald, P. Vieillefosse, and J. P. Hansen, Phys. Rev. Lett. 39, 271 (1977).
[3]J. P. Hansen and I. R. McDonald, *Theory of Simple Liquids* (Academic, London, 1976).
[4]P. Vashista and A. Rahman, Phys. Rev. Lett. 40, 1337 (1978).
[5]M. Baus, Physica (Utrecht) 79A, 377 (1975), and 88A, 319, 336 (1977).
[6]A. A. Barker, Phys. Rev. 171, 186 (1968); C. Deutsch, Phys. Lett. A60, 317 (1977).
[7]S. G. Brush, H. L. Sahlin, and E. Teller, J. Chem. Phys. 45, 2102 (1966).
[8]N. H. March and M. Tosi, *Atomic Dynamics in Liquids* (Macmillan, London, 1976).

Experimental Observation of the Impurity-Flow–Reversal Effect in a Tokamak Plasma

Keith H. Burrell, J. C. DeBoo, E. S. Ensberg, Ronald Prater, and Seung Kai Wong
General Atomic Company, San Diego, California 92138

and

C. E. Bush, R. J. Colchin, P. H. Edmonds, K. W. Hill, R. C. Isler, Thomas C. Jernigan, M. Murakami, and G. H. Neilson
Oak Ridge National Laboratory, Oak Ridge, Tennessee 37830

(Received 5 July 1978)

The inward trasport of a neon test impurity injected into the plasma in the Impurity Study Experiment (ISX) tokamak has been significantly reduced by poloidally asymmetric injection of hydrogen gas into the discharge. The result is consistent with the impurity-flow–reversal effect as predicted by neoclassical transport theory.

The inward transport of impurity ions in tokamak plasmas, which is predicted by neoclassical theory and which was clearly seen in the ATC (adiabatic toroidal compressor) tokamak,[1] poses a major problem. Impurities, especially high-Z impurities, can be quite deleterious to energy confinement in fusion-reactor plasmas. Accordingly, it is of interest to study impurity transport with a view towards methods of impurity control.

Ohkawa[2] has shown that within the Pfirsch-Schlüter framework a poloidally asymmetric source of protons can reduce or reverse the inward transport of impurities, thus providing a method of impurity control. Subsequent calculations[3-5] have generalized this result to include the effect of heat sources, lower collisionality, and general flux-surface geometry. The impurity-flow–reversal experiment was designed to test this neoclassical theory, especially the predictions concerning the asymmetric source terms.

In experiments performed on the Impurity Study Experiment (ISX) tokamak,[6] we have found a substantial alteration of the transport of an injected neon impurity when poloidally localized injection of hydrogen gas is used to produce the asymmetric sources. The observed changes are qualitatively consistent with expectations based on simple theoretical models. More quantitative comparisons will be reported later. If these preliminary indications are confirmed by subsequent experiments, this technique could be the basis for a simple, compact impurity-control technique for tokamak plasmas.

The essence of the flow-reversal effect is the use of poloidally localized sources to alter the parallel proton flows.[2-5] This modifies the proton-impurity friction, thus reducing or, perhaps, reversing the inward impurity transport. Theoretical calculations have shown that in the presence of asymmetric sources the radial flux of an

